



AN OPTIMAL FINITE ELEMENT MESH FOR LINEAR ELASTIC STRUCTURAL ANALYSIS

P.K. Jimack

School of Computer Studies, University of Leeds, United Kingdom

Abstract

This paper investigates the adaptive solution of linear elastic structural analysis problems through re-positioning of the finite element nodal points (r -refinement) using an approach known as the Moving Finite Element method. After a brief introduction to the Moving Finite Element method it is proved that this technique can yield optimal finite element solutions on optimal meshes in the energy norm associated with this problem. Following this there is a discussion of the practical applications of this result in the development of adaptive software, where it is proposed that a combination of r -refinement followed by local h -refinement is likely to be most beneficial. A small number of illustrative examples are included.

1 Introduction

The problem of attempting to find an optimal finite element mesh for performing structural analysis has been considered by numerous authors over the past 20 years or so (see [5], [8], [9] or [23] for example). Many possible approaches have been considered, including methods based on energy minimization (such as [8]) and others based upon geometric considerations (such as [5]). In addition numerous different remeshing techniques have also been considered, based upon either h -refinement ([25]), where extra mesh points are added locally, or r -refinement ([5]), where a fixed number of mesh points are redistributed over the computational domain. Other forms of adaptive analysis have also been considered, such as p -refinement for example (where the degree of the finite element approximation is allowed to increase to obtain higher accuracy, [4]), or various combinations of these. In all cases however the general aim is to improve the quality of the finite element approximation space so as to allow accurate solutions to be reliably found at the lowest possibly computational expense.

In this paper we will consider a remeshing technique based upon the use of r -refinement, with a fixed number of degrees of freedom. The approach that we follow is slightly different to most of the papers cited above since this work is motivated primarily by an analysis ([13], [14]) of a finite element technique that was originally intended for use with transient problems, known as the Moving Finite Element method, due to Miller *et al* ([10], [18] and [19]). This method has been applied to a wide variety of time-dependent problems of both hyperbolic (e.g. [2]) and parabolic (e.g. [16]) nature. The idea behind it, which is explained in more de-

tail in section 2 below, is to produce a finite element scheme in which the mesh deforms continuously with time as the solution evolves. In this work, we obtain solutions to elastostatic structural analysis problems through the use of artificial time-stepping in such a way that the final solution obtained turns out to be an optimal finite element solution on an optimal mesh.

A general form for the usual elastostatic equations of linear elasticity, representing a small displacement, $\underline{u}(\underline{x})$, of a (possibly inhomogeneous) structure initially occupying a domain Ω , may be expressed in Cartesian tensor notation as

$$\frac{\partial}{\partial x_j} [C_{ijkl} \frac{\partial u_k}{\partial x_l}] = -\rho b_i, \quad (1.1)$$

where $\rho(\underline{x})$ is the mass density, $\underline{b}(\underline{x})$ is an external body force and $C_{ijkl}(\underline{x})$ are the components of the fourth order elasticity tensor. The usual summation convention for repeated suffices is employed both here and throughout the rest of the paper, and the elasticity tensor is assumed to have the following symmetries:

$$C_{ijkl} = C_{klij} = C_{jikl} = C_{ijlk}. \quad (1.2)$$

Typical boundary conditions associated with this problem are either displacement conditions, of the form

$$u_i = d_i, \quad (1.3)$$

or traction conditions, of the form

$$n_j C_{ijkl} \frac{\partial u_k}{\partial x_l} = n_j \sigma_{ij} = \theta_i, \quad (1.4)$$

or some combination of these on disjoint portions ∂_d and ∂_θ of the boundary $\partial\Omega$. Further details of these equations or boundary conditions may be found in many standard texts, such as [17, chapter 4] for example.

It is well known (see [12, section 5.6] for example) that a Galerkin finite element approximation to the solution, $\underline{u}(\underline{x})$, of this problem on a given mesh yields a best possible approximation to the true solution on this given mesh in the energy norm

$$\begin{aligned} \|\underline{u}\|_E^2 &= \frac{1}{2} \int_{\Omega} \frac{[\frac{\partial u_i}{\partial x_j} + \frac{\partial u_j}{\partial x_i}]}{2} C_{ijkl} \frac{[\frac{\partial u_k}{\partial x_l} + \frac{\partial u_l}{\partial x_k}]}{2} dV = \\ &= \frac{1}{2} \int_{\Omega} \epsilon_{ij} C_{ijkl} \epsilon_{kl} dV = \frac{1}{2} \int_{\Omega} \epsilon_{ij} \sigma_{ij} dV, \end{aligned} \quad (1.5)$$

where σ_{ij} and ϵ_{ij} are the coefficients of the stress and strain tensors respectively. Another way of expressing this is to say that the finite element solution, \underline{u}^h say, is such that

$$\|\underline{u} - \underline{u}^h\|_E = \inf_{\underline{v} \in S} \|\underline{u} - \underline{v}\|_E, \quad (1.6)$$

where S is the finite element approximation space on the given mesh. That is, the finite element solution is the best possible in terms of the energy norm.

In section 3 of this paper we prove that when the r -refinement approach that is proposed here is applied to the problem (1.1) using artificial time-stepping, then under certain hypotheses it is possible to obtain not only the best finite element solution on a given mesh but also the best possible mesh itself, measured in the energy norm (1.5). In section 4 we give some simple numerical examples and consider the significance of this result in terms of its application to practical software for adaptive structural analysis problems. The paper ends with a brief discussion.

2 The Moving Finite Element Method

As briefly outlined in section 1, one strategy for adaptively solving problem (1.1) is to introduce an artificial time parameter, τ say, and solve the parabolic problem

$$\frac{\partial u_i}{\partial \tau} = \rho b_i + \frac{\partial}{\partial x_j} [C_{ijkl} \frac{\partial u_k}{\partial x_l}] \quad (2.1)$$

on a continuously deforming spatial mesh. Of course in practice the solution will be determined by taking a finite number of discrete "time"-steps and so the solution process itself is not actually that different from a more conventional adaptive strategy involving numerous solution/remeshing iterations, although the underlying philosophy is rather different.

In this section we concentrate on the solution of (2.1) using the Moving Finite Element (MFE) method [3,19]. In the first subsection the MFE method is derived for a more simple linear parabolic problem than (2.1). Section 2.2 then extends this approach to the modified linear elasticity equations of (2.1) in the presence of simple displacement boundary conditions. The affects of more complicated displacement and traction boundary conditions are briefly outlined in section 2.3.

2.1 A Simple Example Problem

In this subsection we give a brief outline of the Moving Finite Element method and how it may be used to solve the following linear evolution equation:

$$\frac{\partial u}{\partial t}(\underline{x}, t) = b(\underline{x}) + \frac{\partial}{\partial x_i} [c_{ij}(\underline{x}) \frac{\partial u}{\partial x_j}(\underline{x}, t)],$$

$$\forall \underline{x} \in \Omega \subseteq \mathfrak{R}^d \text{ and } t \in (0, T]. \quad (2.2)$$

Here we will take $d = 2$ and will assume that the matrix $C(\underline{x})$ is differentiable, symmetric and strictly positive definite. For simplicity we will also assume that the domain Ω is fixed, that its boundary $\partial\Omega$ is polygonal and that on this boundary the solution satisfies the homogeneous Dirichlet condition

$$u|_{\partial\Omega} = 0. \quad (2.3)$$

(It is straightforward to demonstrate existence and uniqueness of a classical solution of (2.2) in this case provided the boundary has no problematic corners (see [11, section 6.3] for example).)

In order to proceed it will be helpful to introduce some notation. It is possible to discretize Ω into a set of non-overlapping triangles which can be uniquely specified as a mesh $\mathcal{M} = (\underline{s}, \mathcal{C})$, where

$$\underline{s} = (\underline{s}_1, \dots, \underline{s}_N, \underline{s}_{N+1}, \dots, \underline{s}_{N+B}) \quad (2.4)$$

is an ordered set of the position vectors of the vertices of the mesh (N interior points and B points on the boundary), and \mathcal{C} is a list of all of the edges. The MFE method seeks to approximate $u(\underline{x}, t)$, the solution of (2.2), by a time-dependent piecewise linear function, u^h say, defined on a mesh of triangles $\mathcal{M}(t) = (\underline{s}(t), \mathcal{C})$ covering the spatial domain Ω . As has been indicated, this mesh is allowed to deform smoothly in time by allowing the positions of the internal knot points, $\underline{s}_1(t), \dots, \underline{s}_N(t)$, to be time-dependent. Their connectivity \mathcal{C} remains fixed however.

Because \mathcal{C} is kept fixed throughout we will generally refer to a mesh $\mathcal{M}(t) = (\underline{s}(t), \mathcal{C})$ only by the ordered set $\underline{s}(t)$ for notational convenience. Given that this is the case we can write our approximation u^h in the form

$$u^h(\underline{x}, t) = \sum_{m=1}^N a_m(t) \alpha_m(\underline{x}, \underline{s}(t)), \quad (2.5)$$

where α_m is the usual continuous piecewise linear "hat" basis function on the mesh $\underline{s}(t)$:

$$\alpha_m(\underline{s}_n(t), \underline{s}(t)) = \delta_{mn}, \quad m = 1, \dots, N; \quad n = 1, \dots, N + B.$$

The sum only goes from 1 to N because of the homogeneous Dirichlet boundary conditions on $\partial\Omega$.

In order to obtain this approximation to $u(\underline{x}, t)$ we need to find values for the unknowns $a_1(t), \underline{s}_1(t), \dots, a_N(t), \underline{s}_N(t)$. The Moving Finite Element method does this by producing a weak or variational form of (2.2) for which the trial solution u^h takes the form of (2.5) and the test space is the space in which the function $\frac{\partial u^h}{\partial t}$ lies at each instant in time. In order to determine this space we differentiate (2.5) with respect to time to give

$$\begin{aligned} \frac{\partial u^h}{\partial t} &= \frac{\partial}{\partial t} \sum_{m=1}^N a_m(t) \alpha_m(\underline{x}, \underline{s}(t)) \\ &= \sum_{m=1}^N \dot{a}_m \alpha_m + \sum_{m=1}^N a_m \nabla_s \alpha_m \cdot \frac{d\underline{s}}{dt}, \end{aligned} \quad (2.6)$$

where the second term arises due to the time-dependence of each α_i through the time-dependence of the mesh \underline{s} , and the gradient operator ∇_s applies to the \underline{s} variables only. Hence

$$\begin{aligned} \frac{\partial u^h}{\partial t} &= \sum_{m=1}^N \dot{a}_m \alpha_m + \nabla_s u^h \cdot \frac{d\underline{s}}{dt} \\ &= \sum_{m=1}^N \dot{a}_m \alpha_m + \sum_{m=1}^N \dot{\underline{s}}_m \cdot \frac{\partial u^h}{\partial \underline{s}_m} \\ &= \sum_{m=1}^N (\dot{a}_m \alpha_m + \dot{\underline{s}}_m \cdot \underline{\beta}_m), \end{aligned} \quad (2.7)$$

where $\underline{\beta}_m = \frac{\partial u^h}{\partial \underline{s}_m} = (\frac{\partial u^h}{\partial s_{m1}}, \frac{\partial u^h}{\partial s_{m2}})^T$ and the dot above a variable denotes differentiation with respect to time.

Lemma 2.1

$$\underline{\beta}_m = \frac{\partial u^h}{\partial \underline{x}_m} = -\alpha_m \nabla u^h,$$

and hence

$$\beta_{md} = -\alpha_m \frac{\partial u^h}{\partial x_d} \quad \text{for } d = 1, 2. \quad (2.8)$$

Proof See [15].

Hence in order to minimize the p.d.e. residual over all possible choices of $\frac{\partial u^h}{\partial t}$ the Moving Finite Element method takes a weak form of (2.2) for which the test space is the space spanned by the functions

$$\{\alpha_1, \beta_{11}, \beta_{12}, \dots, \alpha_N, \beta_{N1}, \beta_{N2}\}.$$

The most straightforward weak form of this type is the simple generalization of the Galerkin method given formally by the differential system

$$\left\langle \sum_{m=1}^N (\dot{a}_m \alpha_m + \dot{\underline{x}}_m \cdot \underline{\beta}_m), \alpha_n \right\rangle = \left\langle b + \frac{\partial}{\partial x_i} [c_{ij} \frac{\partial u^h}{\partial x_j}], \alpha_n \right\rangle \quad (2.9)$$

and

$$\left\langle \sum_{m=1}^N (\dot{a}_m \alpha_m + \dot{\underline{x}}_m \cdot \underline{\beta}_m), \beta_{ne} \right\rangle = \left\langle b + \frac{\partial}{\partial x_i} [c_{ij} \frac{\partial u^h}{\partial x_j}], \beta_{ne} \right\rangle \quad (2.10)$$

for the unknowns $a_1(t), \underline{x}_1(t), \dots, a_N(t), \underline{x}_N(t)$, where the values of $n \in \{1, \dots, N\}$ and $e \in \{1, 2\}$. In the above notation $\langle \cdot, \cdot \rangle$ represents the usual L^2 inner product on Ω .

It should be noted at this point however that the second of these sets of equations is not properly defined for a piecewise linear function $u^h(\underline{x}, t)$, even in a distributional sense. To overcome this difficulty it is necessary to express these equations in a formally equivalent form which is well-defined for such functions u^h . This can be achieved by applying the following integration by parts argument, similar to that in [20], to the second order term on the right-hand-side of (2.10):

$$\begin{aligned} & - \int_{\Omega} \frac{\partial}{\partial x_i} [c_{ij} \frac{\partial u^h}{\partial x_j}] \alpha_n \frac{\partial u^h}{\partial x_e} dV \\ &= \int_{\Omega} c_{ij} \frac{\partial u^h}{\partial x_j} \alpha_n \frac{\partial^2 u^h}{\partial x_i \partial x_e} dV + \int_{\Omega} c_{ij} \frac{\partial u^h}{\partial x_j} \frac{\partial \alpha_n}{\partial x_i} \frac{\partial u^h}{\partial x_e} dV \\ &= \frac{1}{2} \int_{\Omega} \alpha_n c_{ij} \left[\frac{\partial u^h}{\partial x_j} \frac{\partial}{\partial x_e} \left(\frac{\partial u^h}{\partial x_i} \right) + \frac{\partial u^h}{\partial x_i} \frac{\partial}{\partial x_e} \left(\frac{\partial u^h}{\partial x_j} \right) \right] dV \\ & \quad + \int_{\Omega} c_{ij} \frac{\partial u^h}{\partial x_j} \frac{\partial \alpha_n}{\partial x_i} \frac{\partial u^h}{\partial x_e} dV \end{aligned}$$

(where the symmetry $c_{ij} = c_{ji}$ has been used)

$$\begin{aligned} &= \frac{1}{2} \int_{\Omega} \alpha_n c_{ij} \frac{\partial}{\partial x_e} \left[\frac{\partial u^h}{\partial x_i} \frac{\partial u^h}{\partial x_j} \right] dV + \int_{\Omega} c_{ij} \frac{\partial u^h}{\partial x_j} \frac{\partial \alpha_n}{\partial x_i} \frac{\partial u^h}{\partial x_e} dV \\ &= -\frac{1}{2} \int_{\Omega} \frac{\partial u^h}{\partial x_i} \frac{\partial u^h}{\partial x_j} \frac{\partial}{\partial x_e} [\alpha_n c_{ij}] dV + \int_{\Omega} c_{ij} \frac{\partial u^h}{\partial x_j} \frac{\partial \alpha_n}{\partial x_i} \frac{\partial u^h}{\partial x_e} dV. \end{aligned} \quad (2.11)$$

The last line of this expression is defined for piecewise linear functions u^h and so can be used in the definition of the

Moving Finite Element equations (derived from (2.9) and (2.10)):

$$\begin{aligned} & \sum_{m=1}^N \int_{\Omega} \alpha_m \alpha_n dV \dot{a}_m + \sum_{m=1}^N \sum_{d=1}^2 \int_{\Omega} \beta_{md} \alpha_n dV \dot{s}_{md} = \\ & \int_{\Omega} b \alpha_n dV - \int_{\Omega} c_{ij} \frac{\partial u^h}{\partial x_j} \frac{\partial \alpha_n}{\partial x_i} dV \end{aligned} \quad (2.12)$$

and

$$\begin{aligned} & \sum_{m=1}^N \int_{\Omega} \alpha_m \beta_{ne} dV \dot{a}_m + \sum_{m=1}^N \sum_{d=1}^2 \int_{\Omega} \beta_{md} \beta_{ne} dV \dot{s}_{md} = \\ & \int_{\Omega} b \beta_{ne} dV - \frac{1}{2} \int_{\Omega} \frac{\partial u^h}{\partial x_i} \frac{\partial u^h}{\partial x_j} \frac{\partial}{\partial x_e} [\alpha_n c_{ij}] dV \\ & + \int_{\Omega} c_{ij} \frac{\partial u^h}{\partial x_j} \frac{\partial \alpha_n}{\partial x_i} \frac{\partial u^h}{\partial x_e} dV \end{aligned} \quad (2.13)$$

for $n = 1, \dots, N$ and $e = 1, 2$. Note that the use of homogeneous Dirichlet boundary conditions has again simplified things by ensuring that there are no boundary integrals present in these equations. Also, some authors prefer to derive these equations in a slightly different manner, using mollification or recovery methods to deal with the second derivatives (see [7], [16] or [19] for example).

As has already been implied, the sets of equations (2.12) and (2.13) are referred to as the Moving Finite Element equations. They form a system of ordinary differential equations which may be written in the form

$$A(\underline{y}) \dot{\underline{y}} = \underline{g}(\underline{y}), \quad (2.14)$$

where

$$\underline{y} = (a_1, s_{11}, s_{12}, \dots, a_N, s_{N1}, s_{N2})^T,$$

$$\underline{\alpha} = (\alpha_1, \beta_{11}, \beta_{12}, \dots, \alpha_N, \beta_{N1}, \beta_{N2})^T,$$

$$A = \langle \underline{\alpha}, \underline{\alpha}^T \rangle$$

and \underline{g} is the vector of right-hand-sides. The matrix $A(\underline{y})$ is often called the "MFE mass matrix" by analogy with the usual Galerkin mass matrix.

Lemma 2.2 *The matrix $A(\underline{y})$ is positive semi-definite and is singular if and only if the functions in the ordered set $\underline{\alpha}$, defined above, form a linearly dependent set. Further, such a linear dependence can occur if and only if the MFE solution, u^h , has a directional derivative which is continuous at one or more of the knot points $\underline{x}_1, \dots, \underline{x}_N$.*

Proof See [24].

It should be noted that even though (2.2) is linear, the MFE semi-discretization yields a non-linear system of differential equations (2.14). When the matrix $A(\underline{y})$ in this system is singular due to u^h having a continuous directional derivative at a knot point, the MFE solution will be described as "degenerate". Otherwise it will be said to be "non-degenerate", in which case $A(\underline{y})$ is strictly positive definite.

The difficulties associated with degeneracy along with the possibility of the area of one or more of the elements in the mesh becoming non-positive as the knot points evolve are often cited as two of the major drawbacks of the MFE method. One approach to overcoming these difficulties is to attempt to influence the nodal motion by using penalty functions in the underlying minimization to which equations

(2.12) and (2.13) correspond. This is the approach of Miller *et al* ([10], [18], [19]) and Mueller and Carey [21] for example. However, much of the work of Baines *et al* ([1], [2], [3], [16], [24]) suggests that the use of these awkward-to-handle penalty functions may not always be necessary. No such penalty functions will be considered in this paper.

2.2 Using MFE for Linear Elastic Structural Analysis

We now return to equation (2.1) for which we wish to obtain a steady solution using the Moving Finite Element method. This will then give a solution to the original problem (1.1), hopefully on a high quality mesh. Following the approach of subsection 2.1 we will again assume zero Dirichlet (displacement) boundary conditions

$$\underline{u}|_{\partial\Omega} = \underline{0}$$

over the entire boundary $\partial\Omega$. This choice of boundary condition is made in the first instance in order to keep the theory that follows as simple and concise as possible (subsection 2.3 addresses the use of a wider variety of boundary conditions). Also for simplicity we will again work in two space dimensions and assume that our domain has a piecewise linear boundary. Hence, for $i = 1, 2$, we seek an approximation of the form

$$u_i^h(\underline{x}, \tau) = \sum_{m=1}^N a_{mi}(\tau) \alpha_m(\underline{x}, \underline{s}(\tau)), \quad (2.15)$$

where

$$\underline{s}(\tau) = (\underline{s}_1(\tau), \dots, \underline{s}_N(\tau), \underline{s}_{N+1}(\tau), \dots, \underline{s}_{N+B}(\tau)) \quad (2.16)$$

as before. Also, as in (2.6) and (2.7) we can easily deduce that

$$\frac{\partial u_i^h}{\partial \tau} = \sum_{m=1}^N (\dot{a}_{mi} \alpha_m + \dot{\underline{s}}_m \cdot \frac{\partial u_i^h}{\partial \underline{s}_m}) \quad (2.17)$$

where, again using [15],

$$\frac{\partial u_i^h}{\partial \underline{s}_m} = -\alpha_m \nabla u_i^h,$$

and so

$$\frac{\partial u_i^h}{\partial s_{md}} = -\alpha_m \frac{\partial u_i^h}{\partial x_d} \quad \text{for } d = 1, 2. \quad (2.18)$$

Here the dot above a variable denotes differentiation with respect to the variable τ .

Now recall that the Moving Finite Element method seeks to minimize the residual of the p.d.e. (2.1) over all possible choices of $\frac{\partial u_i^h}{\partial \tau}$ by taking a weak form of the equation using a test space that is spanned by the functions

$$\left\{ \alpha_1, \frac{\partial u_i^h}{\partial s_{11}}, \frac{\partial u_i^h}{\partial s_{12}}, \dots, \alpha_N, \frac{\partial u_i^h}{\partial s_{N1}}, \frac{\partial u_i^h}{\partial s_{N2}} \right\},$$

for $i = 1, 2$. This leads to the following differential system:

$$\left\langle \sum_{m=1}^N (\dot{a}_{mi} \alpha_m + \dot{\underline{s}}_m \cdot \frac{\partial u_i^h}{\partial \underline{s}_m}), \alpha_n \right\rangle = \left\langle \rho b_i + \frac{\partial}{\partial x_j} [C_{ijkl} \frac{\partial u_k^h}{\partial x_l}], \alpha_n \right\rangle \quad (2.19)$$

for $i = 1, 2$ and $n = 1, \dots, N$, and

$$\begin{aligned} & \left\langle \sum_{m=1}^N (\dot{a}_{mi} \alpha_m + \dot{\underline{s}}_m \cdot \frac{\partial u_i^h}{\partial \underline{s}_m}), \frac{\partial u_i^h}{\partial s_{ne}} \right\rangle = \\ & \left\langle \rho b_i + \frac{\partial}{\partial x_j} [C_{ijkl} \frac{\partial u_k^h}{\partial x_l}], \frac{\partial u_i^h}{\partial s_{ne}} \right\rangle \end{aligned} \quad (2.20)$$

for $n = 1, \dots, N$ and $e = 1, 2$.

As with equation (2.10) it is again the case that the second order term on the right-hand-side of (2.20) is not properly defined when $u_i^h(\underline{x}, \tau)$ is piecewise linear. Thus, we need to express this as a formally equivalent expression which is well-defined. By noting that

$$\begin{aligned} & - \int_{\Omega} \frac{\partial}{\partial x_j} [C_{ijkl} \frac{\partial u_k^h}{\partial x_l}] \alpha_n \frac{\partial u_i^h}{\partial x_e} dV \\ & = \int_{\Omega} C_{ijkl} \frac{\partial u_k^h}{\partial x_l} \alpha_n \frac{\partial^2 u_i^h}{\partial x_j \partial x_e} dV + \int_{\Omega} C_{ijkl} \frac{\partial u_k^h}{\partial x_l} \frac{\partial \alpha_n}{\partial x_j} \frac{\partial u_i^h}{\partial x_e} dV \\ & = \frac{1}{2} \int_{\Omega} \alpha_n C_{ijkl} \left[\frac{\partial u_k^h}{\partial x_l} \frac{\partial}{\partial x_e} \left(\frac{\partial u_i^h}{\partial x_j} \right) + \frac{\partial u_i^h}{\partial x_j} \frac{\partial}{\partial x_e} \left(\frac{\partial u_k^h}{\partial x_l} \right) \right] dV \\ & \quad + \int_{\Omega} C_{ijkl} \frac{\partial u_k^h}{\partial x_l} \frac{\partial \alpha_n}{\partial x_j} \frac{\partial u_i^h}{\partial x_e} dV \end{aligned}$$

(where the symmetry $C_{ijkl} = C_{klij}$ has been used)

$$\begin{aligned} & = \frac{1}{2} \int_{\Omega} \alpha_n C_{ijkl} \frac{\partial}{\partial x_e} \left[\frac{\partial u_i^h}{\partial x_j} \frac{\partial u_k^h}{\partial x_l} \right] dV + \int_{\Omega} C_{ijkl} \frac{\partial u_k^h}{\partial x_l} \frac{\partial \alpha_n}{\partial x_j} \frac{\partial u_i^h}{\partial x_e} dV \\ & = -\frac{1}{2} \int_{\Omega} \frac{\partial u_i^h}{\partial x_j} \frac{\partial u_k^h}{\partial x_l} \frac{\partial}{\partial x_e} [\alpha_n C_{ijkl}] dV \\ & \quad + \int_{\Omega} C_{ijkl} \frac{\partial u_k^h}{\partial x_l} \frac{\partial \alpha_n}{\partial x_j} \frac{\partial u_i^h}{\partial x_e} dV, \end{aligned} \quad (2.21)$$

we may obtain the following definition of the Moving Finite Element equations for solving (2.1):

$$\begin{aligned} & \sum_{m=1}^N \int_{\Omega} \alpha_m \alpha_n dV \dot{a}_{mi} + \sum_{m=1}^N \sum_{d=1}^2 \int_{\Omega} \frac{\partial u_i^h}{\partial s_{md}} \alpha_n dV \dot{s}_{md} = \\ & \int_{\Omega} \rho b_i \alpha_n dV - \int_{\Omega} C_{ijkl} \frac{\partial u_k^h}{\partial x_l} \frac{\partial \alpha_n}{\partial x_j} dV \end{aligned} \quad (2.22)$$

for $i = 1, 2$ and $n = 1, \dots, N$, and

$$\begin{aligned} & \sum_{m=1}^N \int_{\Omega} \alpha_m \frac{\partial u_i^h}{\partial s_{ne}} dV \dot{a}_{mi} + \sum_{m=1}^N \sum_{d=1}^2 \int_{\Omega} \frac{\partial u_i^h}{\partial s_{md}} \frac{\partial u_i^h}{\partial s_{ne}} dV \dot{s}_{md} = \\ & \int_{\Omega} \rho b_i \frac{\partial u_i^h}{\partial s_{ne}} dV - \frac{1}{2} \int_{\Omega} \frac{\partial u_i^h}{\partial x_j} \frac{\partial u_k^h}{\partial x_l} \frac{\partial}{\partial x_e} [\alpha_n C_{ijkl}] dV \\ & + \int_{\Omega} C_{ijkl} \frac{\partial u_k^h}{\partial x_l} \frac{\partial \alpha_n}{\partial x_j} \frac{\partial u_i^h}{\partial x_e} dV \end{aligned} \quad (2.23)$$

for $n = 1, \dots, N$ and $e = 1, 2$.

Once again these equations may be written as an ordinary differential system in matrix form as

$$A(\underline{y}) \dot{\underline{y}}(\tau) = \underline{g}(\underline{y}), \quad (2.24)$$

where this time

$$\underline{y} = (a_{11}, a_{12}, s_{11}, s_{12}, \dots, a_{N1}, a_{N2}, s_{N1}, s_{N2})^T,$$

$$\underline{\alpha}_1 = (\alpha_1, 0, \frac{\partial u_1^h}{\partial s_{11}}, \frac{\partial u_1^h}{\partial s_{12}}, \dots, \alpha_N, 0, \frac{\partial u_1^h}{\partial s_{N1}}, \frac{\partial u_1^h}{\partial s_{N2}})^T,$$

$$\underline{\alpha}_2 = (0, \alpha_1, \frac{\partial u_2^h}{\partial s_{11}}, \frac{\partial u_2^h}{\partial s_{12}}, \dots, 0, \alpha_N, \frac{\partial u_2^h}{\partial s_{N1}}, \frac{\partial u_2^h}{\partial s_{N2}})^T,$$

$$A = \langle \underline{\alpha}_1, \underline{\alpha}_1^T \rangle + \langle \underline{\alpha}_2, \underline{\alpha}_2^T \rangle$$

and $\underline{g}(\underline{y})$ is another known right-hand-side vector.

Lemma 2.3 *The matrix $A(\underline{y})$ in (2.24) is positive semi-definite and is singular if and only if the MFE solution, \underline{u}^h , has a directional derivative which is continuous at one or more of the knot points $\underline{s}_1, \dots, \underline{s}_N$.*

Proof Note that

$$\frac{\partial u_i}{\partial \tau} = \underline{\alpha}_i^T \underline{\dot{y}} = \underline{\dot{y}}^T \underline{\alpha}_i.$$

Hence for any choice of the vector $\underline{\dot{y}}$ we have

$$0 \leq \int_{\Omega} \left(\frac{\partial \underline{u}^h}{\partial \tau} \right)^2 dV = \int_{\Omega} \underline{\dot{y}}^T \underline{\alpha}_i \underline{\alpha}_i^T \underline{\dot{y}} dV = \underline{\dot{y}}^T \langle \underline{\alpha}_i, \underline{\alpha}_i^T \rangle \underline{\dot{y}} = \underline{\dot{y}}^T A \underline{\dot{y}}$$

so A is indeed positive semi-definite (it can easily be shown to be symmetric).

Now observe that A is singular if and only if there is some vector $\underline{\dot{y}} (\neq 0)$ such that $\frac{\partial \underline{u}^h}{\partial \tau} = \underline{0}$. That is, $\underline{\dot{y}}^T \underline{\alpha}_i = 0$ for both $i = 1$ and $i = 2$. However $\underline{\dot{y}}^T \underline{\alpha}_i$ can be zero (for $\underline{\dot{y}} \neq 0$) if and only if some directional derivative of u_i is continuous at one or more of the nodes $\underline{s}_1(\tau), \dots, \underline{s}_N(\tau)$. Hence A is singular if and only if there is at least one node for which the same directional derivative of both u_1 and u_2 is continuous. ///

Again we will refer to the matrix $A(\underline{y})$ as the "MFE mass matrix" and we will also refer to \underline{u}^h as being "degenerate" or "non-degenerate" depending on whether $A(\underline{y})$ is singular or not respectively.

By solving the system of equations (2.24) for the unknown knot positions, $\underline{s}(\tau)$, and the unknown nodal amplitudes, $(\underline{a}_1(\tau), \dots, \underline{a}_N(\tau))$, it is possible to find both the mesh and the solution for each value of the parameter τ . When a steady state is reached with respect to changes in this parameter, we will have obtained both a mesh and a solution for the original problem of interest (1.1).

2.3 A Wider Selection of Boundary Conditions

In the previous subsection it is demonstrated how the Moving Finite Element method can be applied to the solution of equation (2.1), thus leading to a solution of the elastostatic problem (1.1) on an adapted mesh. For the purposes of simplicity the approach considered above assumes the existence of homogeneous Dirichlet (displacement) boundary conditions everywhere on $\partial\Omega$ and also fixes the location of all of the finite element node points which lie on this domain boundary. Such restrictions are not in fact necessary and the method is quite capable of dealing with any physical boundary conditions of the form (1.3) or (1.4) on different regions of $\partial\Omega$. Moreover, it is also possible to allow the

constrained motion of boundary node points provided they lie within affine regions of the boundary (and so can move along the boundary without distorting the geometry of the domain).

For example, suppose we have traction conditions, (1.4), on some subset, ∂_{θ} say, of $\partial\Omega$. If we do not wish to allow the motion of any of the node points that lie on $\partial\Omega$ then the only additional degrees of freedom that are added to the problem are the displacements at those nodes lying in ∂_{θ} . Let these nodes be numbered $N+1, \dots, N+A$ (where $A < B$ and B is defined as in (2.4) and (2.16)). The Moving Finite Element Equations, (2.22) and (2.23), then become

$$\sum_{m=1}^{N+A} \int_{\Omega} \alpha_m \alpha_n dV \dot{a}_{mi} + \sum_{m=1}^N \sum_{d=1}^2 \int_{\Omega} \frac{\partial u_i^h}{\partial s_{md}} \alpha_n dV \dot{s}_{md} = \int_{\Omega} \rho b_i \alpha_n dV - \int_{\Omega} C_{ijkl} \frac{\partial u_k^h}{\partial x_l} \frac{\partial \alpha_n}{\partial x_j} dV + \int_{\partial_{\theta}} \theta_i \alpha_n dS$$

for $i = 1, 2$ and $n = 1, \dots, N+A$, and

$$\sum_{m=1}^{N+A} \int_{\Omega} \alpha_m \frac{\partial u_i^h}{\partial s_{ne}} dV \dot{a}_{mi} + \sum_{m=1}^N \sum_{d=1}^2 \int_{\Omega} \frac{\partial u_i^h}{\partial s_{md}} \frac{\partial u_i^h}{\partial s_{ne}} dV \dot{s}_{md} = \int_{\Omega} \rho b_i \frac{\partial u_i^h}{\partial s_{ne}} dV - \frac{1}{2} \int_{\Omega} \frac{\partial u_i^h}{\partial x_j} \frac{\partial u_k^h}{\partial x_l} \frac{\partial}{\partial x_e} [\alpha_n C_{ijkl}] dV + \int_{\Omega} C_{ijkl} \frac{\partial u_k^h}{\partial x_l} \frac{\partial \alpha_n}{\partial x_j} \frac{\partial u_i^h}{\partial x_e} dV$$

for $n = 1, \dots, N$ and $e = 1, 2$. These equations can now be written as a differential system which takes the same form as (2.24) and solved accordingly.

To end this section we illustrate how constrained motion of boundary nodes can be incorporated into the method. Suppose for example that the region ∂_{θ} is a subset of a straight line segment of the boundary whose tangential direction is given by the unit vector \hat{i} (in a counter-clockwise sense). Then we may allow each of the nodes numbered $N+1, \dots, N+A$ to move in this direction, i.e. we can allow $\dot{\underline{s}}_i = \dot{s}_i \hat{i}$ for $i = N+1, \dots, N+A$. This means that expression (2.17) becomes

$$\frac{\partial u_i^h}{\partial \tau} = \sum_{m=1}^{N+A} \dot{a}_{mi} \alpha_m + \sum_{m=1}^N \dot{\underline{s}}_m \cdot \frac{\partial u_i^h}{\partial \underline{s}_m} + \sum_{m=N+1}^{N+A} \dot{s}_m (\hat{i} \cdot \frac{\partial u_i^h}{\partial \underline{s}_m})$$

and so the Moving Finite Element equations (2.22) and (2.23) become

$$\sum_{m=1}^{N+A} \int_{\Omega} \alpha_m \alpha_n dV \dot{a}_{mi} + \sum_{m=1}^N \sum_{d=1}^2 \int_{\Omega} \frac{\partial u_i^h}{\partial s_{md}} \alpha_n dV \dot{s}_{md} + \sum_{m=N+1}^{N+A} \int_{\Omega} (\hat{i} \cdot \frac{\partial u_i^h}{\partial \underline{s}_m}) \alpha_n dV \dot{s}_m = \int_{\Omega} \rho b_i \alpha_n dV - \int_{\Omega} C_{ijkl} \frac{\partial u_k^h}{\partial x_l} \frac{\partial \alpha_n}{\partial x_j} dV + \int_{\partial_{\theta}} \theta_i \alpha_n dS$$

for $i = 1, 2$ and $n = 1, \dots, N+A$,

$$\sum_{m=1}^{N+A} \int_{\Omega} \alpha_m \frac{\partial u_i^h}{\partial s_{ne}} dV \dot{a}_{mi} + \sum_{m=1}^N \sum_{d=1}^2 \int_{\Omega} \frac{\partial u_i^h}{\partial s_{md}} \frac{\partial u_i^h}{\partial s_{ne}} dV \dot{s}_{md} + \sum_{m=N+1}^{N+A} \int_{\Omega} (\hat{i} \cdot \frac{\partial u_i^h}{\partial \underline{s}_m}) \frac{\partial u_i^h}{\partial s_{ne}} dV \dot{s}_m =$$

$$\int_{\Omega} \rho b_i \frac{\partial u_i^h}{\partial s_{ne}} dV - \frac{1}{2} \int_{\Omega} \frac{\partial u_i^h}{\partial x_j} \frac{\partial u_k^h}{\partial x_\ell} \frac{\partial}{\partial x_e} [\alpha_n C_{ijkl}] dV + \int_{\Omega} C_{ijkl} \frac{\partial u_k^h}{\partial x_\ell} \frac{\partial \alpha_n}{\partial x_j} \frac{\partial u_i^h}{\partial x_e} dV$$

for $n = 1, \dots, N$ and $e = 1, 2$, and

$$\begin{aligned} & \sum_{m=1}^{N+A} \int_{\Omega} \alpha_m(\hat{\mathbf{x}}) \cdot \frac{\partial u_i^h}{\partial \hat{\mathbf{x}}_n} dV \hat{a}_{mi} \\ & + \sum_{m=1}^N \sum_{d=1}^2 \int_{\Omega} \frac{\partial u_i^h}{\partial s_{md}} (\hat{\mathbf{x}} \cdot \frac{\partial u_i^h}{\partial \hat{\mathbf{x}}_n}) dV \hat{s}_{md} \\ & + \sum_{m=N+1}^{N+A} \int_{\Omega} (\hat{\mathbf{x}} \cdot \frac{\partial u_i^h}{\partial \hat{\mathbf{x}}_m}) (\hat{\mathbf{x}} \cdot \frac{\partial u_i^h}{\partial \hat{\mathbf{x}}_n}) dV \hat{s}_m = \\ & \int_{\Omega} \rho b_i (\hat{\mathbf{x}} \cdot \frac{\partial u_i^h}{\partial \hat{\mathbf{x}}_n}) dV - \frac{1}{2} \int_{\Omega} \hat{\mathbf{x}} \cdot \nabla [\alpha_n C_{ijkl}] \frac{\partial u_i^h}{\partial x_j} \frac{\partial u_k^h}{\partial x_\ell} dV \\ & + \int_{\Omega} C_{ijkl} \frac{\partial u_k^h}{\partial x_\ell} \frac{\partial \alpha_n}{\partial x_j} (\hat{\mathbf{x}} \cdot \nabla u_i^h) dV - \int_{\partial \Omega} \theta_i \alpha_n (\hat{\mathbf{x}} \cdot \nabla u_i^h) dS \end{aligned}$$

for $n = N + 1, \dots, N + A$.

Clearly there are many other combinations of boundary conditions and node motion constraints that could be considered but as is illustrated here they will not particularly effect the underlying nature of the equations that must be solved. For this reason the theory that is developed in the following section is presented only for the simplest case of fixed, zero displacement boundary conditions, (2.3), with (2.24) being the corresponding Moving Finite Element equations. Extensions to cases where there are constrained motions of boundary nodes and/or traction boundary conditions are straightforward.

3 An Optimal Mesh Using the MFE Method

In this section we demonstrate that if the Moving Finite Element method is applied to equation (2.1) in the manner described in subsection 2.2, then it is possible to obtain a steady solution of the MFE equations (2.24) which corresponds to an optimal finite element solution of (1.1) on an *optimal mesh* in the energy norm (1.5). As with subsection 2.2 we will assume here that the boundary conditions associated with (1.1) are zero displacement conditions of the form

$$\mathbf{u}|_{\partial \Omega} = \mathbf{0}.$$

Again this is only for the sake of clarity and all of the theory that we cover in this section can be extended to include more general displacement conditions as well as traction boundary conditions such as those of (1.4).

We begin by defining the following energy functional

$$E(\underline{\varepsilon}) = \frac{1}{2} \int_{\Omega} \frac{\partial e_i}{\partial x_j} C_{ijkl} \frac{\partial e_k}{\partial x_\ell} dV \quad (3.1)$$

and noting that due to the symmetries present in the elasticity tensor (1.2),

$$E(\underline{\varepsilon}) = \|\underline{\varepsilon}\|_E^2,$$

where $\|\cdot\|_E$ is defined in (1.5). The main result of this

section is to show that any stable, steady solution, \underline{y} say, of (2.24) corresponds to a finite element function \underline{u}^h such that the error, $\underline{\varepsilon} = \underline{y} - \underline{u}^h$, is a local minimizer of the energy functional $E(\underline{\varepsilon})$ over all choices of the mesh as well as over all finite element functions on that mesh.

In order to prove this result it will be helpful first to establish some more notation and then to prove a preliminary lemma.

- Suppose $n \in \{1, \dots, N\}$ is the number of an internal node of a triangulation of the domain Ω . Then we will denote by $N(n)$ the number of elements in the triangulation that have this node as a vertex. Further, for $t = 1, \dots, N(n)$, let $T(n, t)$ be a unique ordering of these $N(n)$ elements which have a vertex at \underline{x}_n , let $\Omega_{T(n, t)}$ be the region occupied by the triangle numbered $T(n, t)$ and let $A_{T(n, t)}$ be the area of this region.
- Given any triangle within a finite element mesh we may represent the vertices of that triangle by a local numbering as $\hat{\underline{x}}_0, \hat{\underline{x}}_1$ and $\hat{\underline{x}}_2$.
- We may also define a standard triangle, Δ , as the triangle whose vertices are $\underline{e}_0 = (0, 0)^T$, $\underline{e}_1 = (1, 0)^T$ and $\underline{e}_2 = (0, 1)^T$.
- Now define a mapping from an arbitrary element of a triangulation onto that standard triangle by

$$\underline{\xi}(\underline{x}, \underline{\varepsilon}) = \sum_{\mu=0}^2 \underline{e}_\mu \hat{\alpha}_\mu(\underline{x}, \underline{\varepsilon}) \quad (3.2)$$

where $\hat{\alpha}_\mu(\underline{x}, \underline{\varepsilon})$ is the usual linear basis function (but with a local numbering corresponding to a particular triangle) such that $\hat{\alpha}_\mu(\underline{e}_\nu, \underline{\varepsilon}) = \delta_{\mu\nu}$, for $\mu, \nu \in \{0, 1, 2\}$.

- The inverse of this mapping is

$$\underline{x}(\underline{\xi}, \underline{\varepsilon}) = \sum_{\mu=0}^2 \hat{\underline{x}}_\mu \bar{\alpha}_\mu(\underline{\xi}) \quad (3.3)$$

where the $\bar{\alpha}_\mu(\underline{\xi})$ are the piecewise linear basis functions on the standard triangle such that $\bar{\alpha}_\mu(\underline{e}_\nu) = \delta_{\mu\nu}$. (Note that $\bar{\alpha}_\mu(\underline{\xi}) \equiv \hat{\alpha}_\mu(\underline{x}(\underline{\xi}, \underline{\varepsilon}), \underline{\varepsilon})$.)

Lemma 3.1 Given a triangle with vertices $\hat{\underline{x}}_0, \hat{\underline{x}}_1, \hat{\underline{x}}_2$ and area $A(\hat{\underline{x}}_0, \hat{\underline{x}}_1, \hat{\underline{x}}_2)$, then

$$\frac{\partial A}{\partial \hat{s}_{\nu e}} = \frac{\partial \hat{\alpha}_\nu}{\partial x_e} A \quad \text{for } \nu \in \{0, 1, 2\} \text{ and } e \in \{1, 2\}.$$

Proof Without loss of generality consider the case $\nu = 0$. Because each of $\hat{\alpha}_0, \hat{\alpha}_1$ and $\hat{\alpha}_2$ are area coordinates we know that

$$\hat{\alpha}_0(\underline{x}) = A(\underline{x}, \hat{\underline{x}}_1, \hat{\underline{x}}_2) / A(\hat{\underline{x}}_0, \hat{\underline{x}}_1, \hat{\underline{x}}_2). \quad (3.4)$$

Moreover, since $\hat{\alpha}_0$ is affine we know that $\frac{\partial \hat{\alpha}_0}{\partial x_e}$ is independent of \underline{x} and so from (3.4) $\frac{\partial}{\partial x_e} A(\underline{x}, \hat{\underline{x}}_1, \hat{\underline{x}}_2)$ must be independent of \underline{x} . This implies that $\frac{\partial}{\partial \hat{s}_{0e}} A(\hat{\underline{x}}_0, \hat{\underline{x}}_1, \hat{\underline{x}}_2)$ must be independent of $\hat{\underline{x}}_0$ and therefore that

$$\frac{\partial}{\partial x_e} A(\underline{x}, \hat{\underline{x}}_1, \hat{\underline{x}}_2) = \frac{\partial}{\partial \hat{s}_{0e}} A(\hat{\underline{x}}_0, \hat{\underline{x}}_1, \hat{\underline{x}}_2).$$

Hence

$$\frac{\partial \hat{\alpha}_0}{\partial x_e} = \frac{\partial A}{\partial \hat{s}_{0e}} / A.$$

Since this argument is valid for any choice of $\nu \in \{0, 1, 2\}$, the result is proved. //

We are now in a position to prove the following theorem.

Theorem 3.2 Let $\underline{U}(\underline{x})$ be the unique steady solution of (2.1) subject to homogeneous Dirichlet boundary conditions on $\partial\Omega$ (i.e. the unique solution of (1.1) subject to these boundary conditions - see [6, section 2.2] for a proof that such a function exists). Also let

$$\underline{u}^h(\underline{x}, \tau) = \sum_{m=1}^N \underline{a}_m(\tau) \alpha_m(\underline{x}, \underline{s}(\tau))$$

be a continuous piecewise linear approximation to $\underline{U}(\underline{x})$ on a mesh $\underline{s}(\tau)$ with N free internal knots $\underline{s}_1(\tau), \dots, \underline{s}_N(\tau)$. Also let

$$\underline{y} = (a_{11}, a_{12}, s_{11}, s_{12}, \dots, a_{N1}, a_{N2}, s_{N1}, s_{N2})^T$$

and $I(\underline{y}) = E(\underline{s})$ where E is defined by (3.1) with $\underline{s} = \underline{U} - \underline{u}^h$. Then

$$\nabla I(\underline{y}) = -\underline{g}(\underline{y}), \quad (3.5)$$

for $\underline{g}(\underline{y})$ as in (2.24).

Proof We begin by observing, from (2.22) and (2.23), that $\underline{g}(\underline{y})$ consists of the following components:

$$\int_{\Omega} \rho b_i \alpha_n dV - \int_{\Omega} C_{ijkl} \frac{\partial u_k^h}{\partial x_l} \frac{\partial \alpha_n}{\partial x_j} dV \quad (3.6)$$

for $i = 1, 2$ and $n = 1, \dots, N$, and

$$\int_{\Omega} \rho b_i \frac{\partial u_i^h}{\partial s_{ne}} dV - \frac{1}{2} \int_{\Omega} \frac{\partial u_i^h}{\partial x_j} \frac{\partial u_k^h}{\partial x_l} \frac{\partial}{\partial x_e} [\alpha_n C_{ijkl}] dV + \int_{\Omega} C_{ijkl} \frac{\partial u_k^h}{\partial x_l} \frac{\partial \alpha_n}{\partial x_j} \frac{\partial u_i^h}{\partial x_e} dV \quad (3.7)$$

for $n = 1, \dots, N$ and $e = 1, 2$. We now show that the components of $\nabla I(\underline{y})$ are as claimed in (3.5) by demonstrating that (3.6) is $-\frac{\partial I}{\partial a_{ni}}$ for $i = 1, 2$ and $n = 1, \dots, N$, and (3.7) is $-\frac{\partial I}{\partial s_{ne}}$ for $n = 1, \dots, N$ and $e = 1, 2$.

For the first of these two cases,

$$\begin{aligned} \frac{\partial I}{\partial a_{ni}} &= \frac{1}{2} \frac{\partial}{\partial a_{ni}} \int_{\Omega} \frac{\partial}{\partial x_j} (U_g - u_g^h) C_{gjk\ell} \frac{\partial}{\partial x_\ell} (U_k - u_k^h) dV \\ &= -\frac{1}{2} \int_{\Omega} \frac{\partial}{\partial x_j} (U_g - u_g^h) C_{gjk\ell} \delta_{ik} \frac{\partial \alpha_n}{\partial x_\ell} dV \\ &\quad - \frac{1}{2} \int_{\Omega} \delta_{ig} \frac{\partial \alpha_n}{\partial x_j} C_{gjk\ell} \frac{\partial}{\partial x_\ell} (U_k - u_k^h) dV \\ &= - \int_{\Omega} \delta_{ig} \frac{\partial \alpha_n}{\partial x_j} C_{gjk\ell} \frac{\partial}{\partial x_\ell} (U_k - u_k^h) dV \\ &\quad \text{(using the symmetry } C_{gjk\ell} = C_{k\ell gj}\text{)} \\ &= \int_{\Omega} \frac{\partial \alpha_n}{\partial x_j} C_{ijk\ell} \frac{\partial u_k^h}{\partial x_\ell} dV - \int_{\Omega} \frac{\partial \alpha_n}{\partial x_j} C_{ijk\ell} \frac{\partial U_k}{\partial x_\ell} dV \\ &= \int_{\Omega} \frac{\partial \alpha_n}{\partial x_j} C_{ijk\ell} \frac{\partial u_k^h}{\partial x_\ell} dV + \int_{\Omega} \alpha_n \frac{\partial}{\partial x_j} [C_{ijk\ell} \frac{\partial U_k}{\partial x_\ell}] dV \\ &= \int_{\Omega} \frac{\partial \alpha_n}{\partial x_j} C_{ijk\ell} \frac{\partial u_k^h}{\partial x_\ell} dV - \int_{\Omega} \alpha_n \rho b_i dV, \quad (3.8) \end{aligned}$$

which is equal to -1 times (3.6) as required.

For the other case

$$\begin{aligned} \frac{\partial I}{\partial s_{ne}} &= \frac{1}{2} \frac{\partial}{\partial s_{ne}} \int_{\Omega} \frac{\partial}{\partial x_j} (U_i - u_i^h) C_{ijk\ell} \frac{\partial}{\partial x_\ell} (U_k - u_k^h) dV \\ &= \frac{1}{2} \frac{\partial}{\partial s_{ne}} \int_{\Omega} \frac{\partial u_i^h}{\partial x_j} C_{ijk\ell} \frac{\partial u_k^h}{\partial x_\ell} dV \\ &\quad - \frac{\partial}{\partial s_{ne}} \int_{\Omega} \frac{\partial u_i^h}{\partial x_j} C_{ijk\ell} \frac{\partial U_k}{\partial x_\ell} dV \\ &\quad \text{(using the symmetry } C_{ijk\ell} = C_{k\ell ij}\text{)} \\ &= \frac{1}{2} \frac{\partial}{\partial s_{ne}} \sum_{t=1}^{N(n)} \int_{\Omega_{T(n,t)}} \frac{\partial u_i^h}{\partial x_j} C_{ijk\ell} \frac{\partial u_k^h}{\partial x_\ell} dV \\ &\quad + \frac{\partial}{\partial s_{ne}} \int_{\Omega} u_i^h \frac{\partial}{\partial x_j} [C_{ijk\ell} \frac{\partial U_k}{\partial x_\ell}] dV \\ &= \frac{1}{2} \sum_{t=1}^{N(n)} \frac{\partial}{\partial \hat{s}_{\nu e}} \int_{\Delta} D_{ij} C_{ijk\ell}(\underline{x}(\underline{\xi}, \underline{s})) D_{k\ell} \left| \frac{d\underline{x}}{d\underline{\xi}} \right| d\underline{\xi} \\ &\quad - \frac{\partial}{\partial s_{ne}} \int_{\Omega} u_i^h \rho b_i dV, \end{aligned}$$

where on each triangle, $T(n, t)$, ν is the local vertex number corresponding to node n and D_{pq} represents the value of $\frac{\partial u_p^h}{\partial x_q}$ restricted to this triangle (note that this value is independent of \underline{x} since we are using piecewise linear finite elements). Also noting that on each triangle, $T(n, t)$, the Jacobian, $\left| \frac{d\underline{x}}{d\underline{\xi}} \right|$, of the transformation (3.2) onto the standard triangle, Δ , is simply $2A_{T(n,t)}$, we deduce that,

$$\begin{aligned} \frac{\partial I}{\partial s_{ne}} &= \frac{1}{2} \sum_{t=1}^{N(n)} \int_{\Delta} \{ [D_{ij} C_{ijk\ell} D_{k\ell}] 2 \frac{\partial}{\partial \hat{s}_{\nu e}} A_{T(n,t)} + \\ &\quad [D_{ij} D_{k\ell} \frac{\partial C_{ijk\ell}}{\partial \underline{x}} \cdot \frac{\partial \underline{x}}{\partial \hat{s}_{\nu e}} \\ &\quad + C_{ijk\ell} \frac{\partial}{\partial \hat{s}_{\nu e}} (D_{ij} D_{k\ell})] 2A_{T(n,t)} \} d\underline{\xi} \\ &\quad - \frac{\partial}{\partial s_{ne}} \int_{\Omega} u_i^h \rho b_i dV \\ &= \frac{1}{2} \sum_{t=1}^{N(n)} \int_{\Delta} \{ [D_{ij} C_{ijk\ell} D_{k\ell}] \frac{\partial \hat{\alpha}_\nu}{\partial x_e} + [D_{ij} D_{k\ell} \frac{\partial C_{ijk\ell}}{\partial x_e} \hat{\alpha}_\nu] + \\ &\quad C_{ijk\ell} [D_{ij} \frac{\partial}{\partial x_\ell} (\frac{\partial u_k^h}{\partial \hat{s}_{\nu e}}) \\ &\quad + D_{k\ell} \frac{\partial}{\partial x_j} (\frac{\partial u_i^h}{\partial \hat{s}_{\nu e}})] \} 2A_{T(n,t)} d\underline{\xi} \\ &\quad - \int_{\Omega} \frac{\partial u_i^h}{\partial s_{ne}} \rho b_i dV \\ &\quad \text{(using lemma 3.1 and equation (3.3))} \\ &= \frac{1}{2} \sum_{t=1}^{N(n)} \int_{\Delta} \{ [D_{ij} C_{ijk\ell} D_{k\ell}] \frac{\partial \hat{\alpha}_\nu}{\partial x_e} + [D_{ij} D_{k\ell} \frac{\partial C_{ijk\ell}}{\partial x_e} \hat{\alpha}_\nu] - \\ &\quad C_{ijk\ell} [D_{ij} \frac{\partial}{\partial x_\ell} (\alpha_\nu D_{ke}) \\ &\quad + D_{k\ell} \frac{\partial}{\partial x_j} (\alpha_\nu D_{ie})] \} 2A_{T(n,t)} d\underline{\xi} \\ &\quad - \int_{\Omega} \frac{\partial u_i^h}{\partial s_{ne}} \rho b_i dV \\ &\quad \text{(using equation (2.18))} \end{aligned}$$

4 Practical Application of the MFE Method in Structural Analysis

As with subsection 2.2, the results of the previous section may easily be generalized to a wider variety of boundary conditions. In particular the result showing how the Moving Finite Element method can lead to a best free-knot linear spline approximation to the solution of (1.1) also holds in conjunction with traction boundary conditions of the form (1.4). Before we demonstrate this computationally however we consider a simple, although rather artificial, example which has a known solution with which we may compare our computed solution in order to verify the result of theorem 3.2 and its corollary.

In this first example the domain, Ω , is $(0, 1) \times (0, 1)$ and the elasticity tensor, C , corresponds to an isotropic material with Young's modulus $E = 100$ and Poisson ratio $\nu = 0.001$. The values of $\rho b_1(\underline{x})$ and $\rho b_2(\underline{x})$ in (1.1) are chosen so as to obtain the exact solution

$$u_1(\underline{x}) = u_2(\underline{x}) = 64x_1^2(1-x_1)x_2^2(1-x_2)$$

which satisfies the zero displacement boundary condition everywhere on $\partial\Omega$. Figure 1 shows the initial and final meshes when a solution to this problem was computed using the Moving Finite Element method and table 1 shows the final values of all of the degrees of freedom (node positions, \underline{x}_i , and displacements, \underline{a}_i , for $i = 1, \dots, 25$). Once these values were obtained we used the NAG library minimization rou-

$$\begin{aligned} &= \frac{1}{2} \sum_{i=1}^{N(n)} \int_{\Omega_{T(n,i)}} \left\{ \left[\frac{\partial u_i^h}{\partial x_j} C_{ijkl} \frac{\partial u_k^h}{\partial x_l} \right] \frac{\partial \alpha_n}{\partial x_e} \right. \\ &\quad \left. + \left[\frac{\partial u_i^h}{\partial x_j} \frac{\partial u_k^h}{\partial x_l} \frac{\partial C_{ijkl}}{\partial x_e} \alpha_n \right] \right. \\ &\quad \left. - 2C_{ijkl} \frac{\partial u_i^h}{\partial x_e} \frac{\partial u_k^h}{\partial x_l} \frac{\partial \alpha_n}{\partial x_j} \right\} dV \\ &\quad - \int_{\Omega} \frac{\partial u_i^h}{\partial s_{ne}} \rho b_i dV \\ &\quad \text{(using the symmetry } C_{ijkl} = C_{klij}) \\ &= \frac{1}{2} \int_{\Omega} \frac{\partial u_i^h}{\partial x_j} \frac{\partial u_k^h}{\partial x_l} \frac{\partial}{\partial x_e} (\alpha_n C_{ijkl}) dV \\ &\quad - \int_{\Omega} C_{ijkl} \frac{\partial u_i^h}{\partial x_e} \frac{\partial u_k^h}{\partial x_l} \frac{\partial \alpha_n}{\partial x_j} dV \\ &\quad - \int_{\Omega} \frac{\partial u_i^h}{\partial s_{ne}} \rho b_i dV, \end{aligned} \quad (3.9)$$

which is equal to -1 times (3.7) as required. ///

The above theorem tells us that when we have obtained a non-degenerate steady solution of the Moving Finite Element Equations (2.24), and so $\underline{g}(\underline{y}) = \underline{0}$, then we are also at a stationary value of the functional $I(\underline{y})$, which is equal to the energy of the error $\underline{U} - \underline{u}^h$. In order to show that this stationary point is in fact a local energy minimizer we must also show that the Hessian of I is positive definite at this point. This means that the Jacobian of $\underline{g}(\underline{y})$, which by (3.5) must be symmetric, must be shown to be negative definite at such a steady solution of the Moving Finite Element equations. This is done in the following proof.

Corollary 3.3 Any non-degenerate, asymptotically stable, steady solution of the MFE equations (2.24) for solving the problem (2.1) is an optimal finite element solution of the elastostatic problem (1.1) on an optimal mesh in the energy norm (1.5)

Proof Suppose \underline{y}_0 is such a non-degenerate, asymptotically stable, steady solution of (2.24), then $A(\underline{y}_0)$ is positive definite (by lemma 2.3). Now take a small perturbation of \underline{y}_0 , given by $\underline{y}_0 + \epsilon \underline{y}_1$, so that (2.24) becomes

$$A(\underline{y}_0 + \epsilon \underline{y}_1)(\dot{\underline{y}}_0 + \epsilon \dot{\underline{y}}_1) = \underline{g}(\underline{y}_0 + \epsilon \underline{y}_1).$$

Linearizing this about \underline{y}_0 gives

$$\dot{\underline{y}}_1 = A^{-1}(\underline{y}_0) D\underline{g}(\underline{y}_0) \underline{y}_1,$$

where $D\underline{g}(\underline{y}_0)$ is the Jacobian of \underline{g} with respect to \underline{y} evaluated at \underline{y}_0 . Now, the asymptotic stability of \underline{y}_0 implies that all eigenvalues of the product $A^{-1}(\underline{y}_0) D\underline{g}(\underline{y}_0)$ must have strictly negative real parts. Since $A^{-1}(\underline{y}_0)$ is strictly positive definite we deduce that $D\underline{g}(\underline{y}_0)$ must be strictly negative definite and so, from (3.5), the Hessian of $I(\underline{y})$ must be strictly positive definite at \underline{y}_0 , as required. ///

The outcome of this therefore means that if we apply the approach outlined in subsection 2.2 to solving the problem (1.1), then any steady solution of (2.24) that we obtain will be locally optimal on an optimal mesh in the energy norm (1.5).

\underline{x}_i	\underline{a}_i
(0.69364970, 0.69364970)	(1.3550871, 1.3550871)
(0.22589896, 0.91261447)	(0.18986173, 0.19742885)
(0.59090799, 0.59090799)	(1.2750743, 1.2750743)
(0.91261447, 0.22589896)	(0.19742885, 0.18986173)
(0.80526143, 0.80526143)	(1.0431178, 1.0431178)
(0.53865798, 0.69448498)	(1.2403749, 1.2463933)
(0.60966146, 0.75403842)	(1.2843933, 1.2818275)
(0.65144442, 0.65144442)	(1.3733659, 1.3733659)
(0.14283922, 0.95538455)	(0.044817489, 0.044377864)
(0.12260433, 0.75885079)	(0.11494611, 0.11378281)
(0.14819209, 0.43261430)	(0.14421655, 0.14233981)
(0.25397459, 0.25397459)	(0.13040246, 0.13040246)
(0.69448498, 0.53865798)	(1.2463933, 1.2403749)
(0.75403842, 0.60966146)	(1.2818275, 1.2843933)
(0.43261430, 0.14819209)	(0.14233981, 0.14421655)
(0.75885079, 0.12260433)	(0.11378281, 0.11494611)
(0.95538455, 0.14283922)	(0.044377864, 0.044817489)
(0.81816556, 0.64261816)	(1.1445529, 1.1530219)
(0.73657273, 0.73657273)	(1.2926651, 1.2926651)
(0.64261816, 0.81816556)	(1.1530219, 1.1445529)
(0.96515183, 0.34947743)	(0.17348793, 0.16987146)
(0.89237610, 0.69457314)	(0.80121411, 0.81922981)
(0.96278242, 0.96278242)	(0.15449516, 0.15449516)
(0.69457314, 0.89237610)	(0.81922981, 0.80121411)
(0.34947743, 0.96515183)	(0.16987146, 0.17348793)

Table 1: The values of the 100 degrees of freedom at the steady MFE solution to the first example problem.

tine E04JAF, [22], to confirm that they do indeed minimize the error (which is known exactly for this example) in the energy norm (1.5). In fact the error in the Moving Finite Element solution is about 20% smaller than the error obtained by a conventional finite element analysis on the original grid (the top grid in figure 1).

Having established the correctness of the results in section 3 for the example above, we now show how the method performs on a slightly more realistic problem which involves the use of traction boundary conditions. Figure 2 depicts an overhanging cantilever beam with a vertical concentrated load at the end of the cantilever. An initial finite element mesh is also shown. When this problem is solved using the same elasticity tensor as in the previous example we obtain the final solution tabulated in table 2, with the corresponding final mesh shown in figure 3.

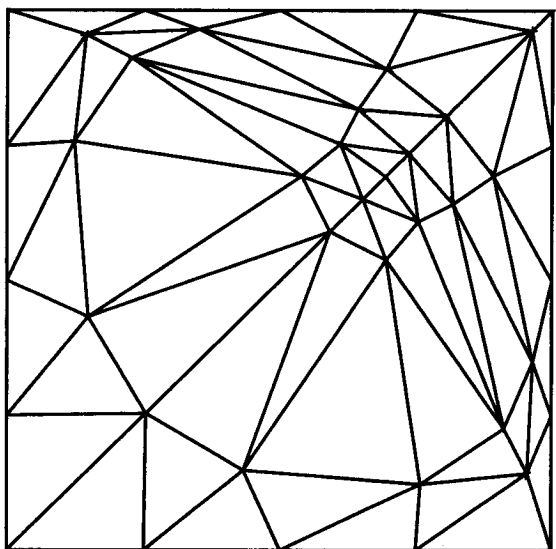
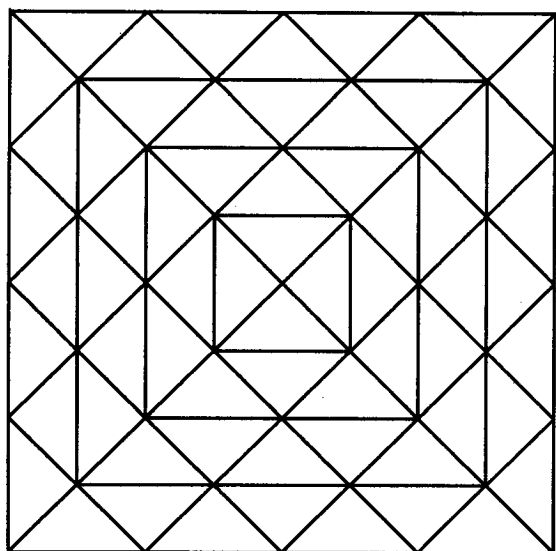


Figure 1: The initial and final meshes in the first example.

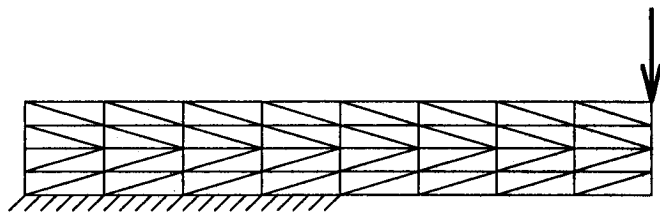


Figure 2: The initial mesh for an overhanging cantilever beam with a vertical concentrated load at the end of the cantilever (the second example).

g_i	u_i
(0.61456606, 0.47923320)	(0.0057128317, 0.0024057717)
(1.3508914, 0.33709922)	(0.018124359, 0.0039853696)
(1.6658348, 0.39799753)	(0.034182316, 0.0039527141)
(1.9843904, 0.51931928)	(0.083173394, -0.020636952)
(2.2980489, 0.43062728)	(0.093319382, -0.11889211)
(2.5632998, 0.48729489)	(0.13994718, -0.24150486)
(2.9466186, 0.42107679)	(0.12854469, -0.49384140)
(0.55265310, 0.26833740)	(0.0040340932, 0.0014452070)
(0.98419625, 0.25049591)	(0.0083095121, 0.0028406895)
(1.6552233, 0.25631920)	(0.019191152, 0.0025423956)
(1.9466160, 0.25760568)	(0.027981717, -0.013151568)
(2.1329383, 0.23533503)	(0.025296867, -0.054448789)
(2.4721697, 0.26354485)	(0.026298447, -0.19275032)
(2.8670582, 0.29304043)	(0.037755895, -0.43405716)
(0.54078305, 0.039875678)	(0.00084279350, 0.00033244597)
(1.2195241, 0.10503114)	(0.0053202886, 0.0010113499)
(1.7953244, 0.13322287)	(0.0096274066, 0.00040332311)
(1.9952269, 0.037836236)	(0.00094441866, -0.0036342981)
(2.2766370, 0.10919590)	(-0.024969937, -0.10738732)
(2.5329448, 0.086488793)	(-0.067484112, -0.22341877)
(2.9324739, 0.19241566)	(-0.033494436, -0.48334012)
(0.0, 0.60)	(0.0030501201, 0.0014523155)
(0.5, 0.60)	(0.0046166793, 0.0025083792)
(1.0, 0.60)	(0.013060042, 0.0045300761)
(1.5, 0.60)	(0.033228801, 0.0072372634)
(2.0, 0.60)	(0.10004046, -0.020532766)
(2.5, 0.60)	(0.19505958, -0.20246448)
(3.0, 0.60)	(0.25710490, -0.53272069)
(3.5, 0.60)	(0.26893202, -0.92149933)
(4.0, 0.60)	(0.27413503, -1.3156280)
(0.0, 0.45)	(0.0031526205, 0.0014838105)
(4.0, 0.45)	(0.15685043, -1.3097350)
(0.0, 0.30)	(0.0025270661, 0.0013058087)
(4.0, 0.30)	(0.042305854, -1.3076245)
(0.0, 0.15)	(0.0014285077, 0.00090359659)
(4.0, 0.15)	(-0.71807578, -1.3068212)
(2.5, 0.00)	(-0.11364067, -0.20379047)
(3.0, 0.00)	(-0.17115245, -0.53300436)
(3.5, 0.00)	(-0.18317899, -0.92003269)
(4.0, 0.00)	(-0.18710608, -1.3067605)

Table 2: The values of the 122 degrees of freedom at the steady MFE solution to the second example problem.

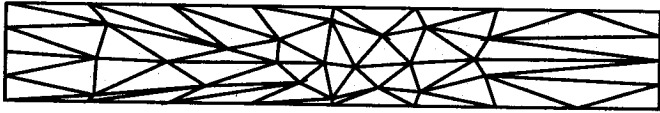


Figure 3: The final mesh in the second example.

At first sight this mesh appears to be of slightly dubious quality however it is possible to confirm that it is indeed optimal even though, unlike the previous example, we have no analytic expression for the exact solution, u . This may be done by observing that since equation (1.1) is linear, any finite element function, u^h , which minimizes the error, $u - u^h$, in the energy norm must itself be a minimizer of the corresponding energy functional. In other words, theorem 3.2 also implies that the steady Moving Finite Element solution, u^h , given in table 2 should be a minimizer of the functional

$$E(\underline{u}^h) = \frac{1}{2} \int_{\Omega} \frac{\partial u_i^h}{\partial x_j} C_{ijkl} \frac{\partial u_k^h}{\partial x_l} dV - \int_{\Omega} \rho b_i u_i dV - \int_{\partial_{\theta}} \theta_i u_i dS, \quad (4.1)$$

where the traction boundary conditions (1.4) hold on $\partial_{\theta} \subset \partial\Omega$. Once more the use of NAG routine E04JAF confirms that the solution obtained is indeed a minimizer of (4.1) over all choices of nodal positions, \underline{g}_i , and displacements, \underline{a}_i .

The reason that the optimal mesh shown in figure 3 may not appear at first sight to be particularly ideal is that it is subject to the constraint of having the same topology as the initial mesh shown in figure 2. This is undoubtedly one of the practical drawbacks of the Moving Finite Element method as outlined here, although the situation is likely to be improved somewhat by remeshing the node points obtained at this stage, thus altering the connectivity, \mathcal{C} , of the grid. (In addition, in this particular example node movement is restricted to those points inside the domain Ω and so there is a lot of stretching of elements adjacent to the boundary. This could be rectified by permitting constrained motion of the boundary nodes as outlined in subsection 2.3.)

Another practical drawback of using the Moving Finite Element method as described in section 2 is the computational overhead associated with it. By allowing the nodal positions to become degrees of freedom we effectively double the size of the discrete problem that must be solved. Moreover, since equations (2.24) are nonlinear and dependent upon the artificial parameter τ , the work involved in solving them is considerably more than that associated with a more conventional discretization of (1.1). This does not mean however that the method and the results of section 3 cannot be of significant practical value.

Firstly, there is no need to solve equations (2.24) with particularly high accuracy: a nearly steady solution (within a couple of percent of the true steady solution for example) will provide an almost optimal mesh, and a good initial estimate of the displacements, which can be used with a standard finite element analysis code. This will allow a considerably more accurate solution to be obtained than would be possible on a uniform mesh.

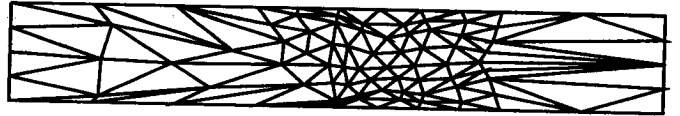


Figure 4: The effect of local h -refinement on the final mesh in the second example.

Secondly, and perhaps more practically, equations (2.24) need only be solved using a coarse finite element mesh. This would yield an optimal coarse initial mesh upon which to base an adaptive finite element analysis using h -refinement. Since the efficiency of most h -refinement algorithms is heavily dependent upon the choice of coarse mesh that is used and it is known that this coarse mesh is optimal, it is to be expected that this combination of r - and h -refinement should work well. Figure 4 illustrates how this looks in practice by showing the effect of local h -refinement on the grid that was produced in the solution to example 2 (figure 3) above. Those elements with the largest contributions to (4.1) have been found at very little extra computational cost and then locally refined, to give the mesh shown. A more accurate solution can now be found on this mesh in the usual way.

5 Discussion

The main result of this paper is a theoretical one which shows that the Moving Finite Element method can be applied to the solution of linear elastic structural analysis problems to yield an optimal solution on an optimal mesh. For clarity the theory is presented for two-dimensional problems however it extends to three dimensions without any fundamental alterations. In addition, although the computational examples discussed in section 4 are for isotropic materials this is not a necessary assumption.

It would be desirable to extend the results to the case of nonlinear structural analysis problems and current research suggests that this is possible. The generalization to nonlinear problems comes from the observation made in section 4 that, for a linear problem, minimizing the error in the energy norm corresponds to minimizing the energy functional (4.1). This leads one to the hypothesis that for problems in nonlinear elasticity the Moving Finite Element method could be used to obtain an optimal mesh for the purposes of energy minimization.

Whilst theoretical results are of interest in their own right, from a practical point of view it is important that they can be utilized to improve the quality of numerical software. It remains to be seen whether the Moving Finite Element method has a role to play in structural analysis however if it does then it will almost certainly be in conjunction with some other form of adaptivity. In section 4 it is suggested that the method could be effectively combined with local h -refinement in order to get an optimal coarse mesh as the starting point for this local refinement. Further work is certainly required to establish the quantitative benefits of this or similar approaches.

A final point which has not been addressed at all in this paper is that of what should be done if the solution of equations (2.24) is such that one or more of the finite elements shrinks to zero area as τ evolves. In theory there is nothing to prevent such an occurrence although this does not appear to happen in practice. It would be useful either to prove that this will never happen or else to implement a suitable strategy, such as regridding the mesh points, for when it does occur.

References

- [1] M J Baines (1985). *Locally Adaptive Moving Finite Elements*. Numerical Methods for Fluid Dynamics II (eds. K W Morton & M J Baines), Oxford University Press.
- [2] M J Baines and A J Wathen (1986). *Moving Finite Element Modelling of Compressible Flow*. Applied Num. Maths., 2, 495–514.
- [3] M J Baines and A J Wathen (1988). *Moving Finite Element Methods for Evolutionary Problems. I. Theory*. J. of Comp. Phys., 79, 245–269.
- [4] I Babuška, B Szabó and I N Katz (1981). *The p-version of the Finite Element Method*. SIAM J. Num. Anal., 18, 515–545.
- [5] Jung-Ho Cheng (1993). *Adaptive Grid Optimization for Structural Analysis – Geometry-Based Approach*. Comput. Meth. Appl. Mech. Eng., 107, 1–22.
- [6] P G Ciarlet (1983). *Lectures on Three Dimensional Elasticity*. Springer-Verlag.
- [7] J D P Donnelly (1990). *Approximation of the Diffusion Term in the Method of Moving Finite Elements*. Oxford University Computing Laboratory Report 90/9. Unpublished.
- [8] C A Fellipa (1976). *Optimization of Finite Element Grids by Direct Energy Search*. App. Math. Modelling, 1, 93–96.
- [9] C A Fellipa (1977). *Numerical Experiments in Finite Element Grid Optimization by Direct Energy Search*. App. Math. Modelling, 1, 231–244.
- [10] R J Gelinias, S K Doss and K Miller (1981). *The Moving Finite Element Method: Application to General Partial Differential Equations with Multiple Large Gradients*. J. of Comp. Phys., 40, 202–249.
- [11] D Gilbarg and N S Trudinger (1983). *Elliptic Partial Differential Equations of Second Order*. Grundlehren der mathematischen Wissenschaften 224, Springer-Verlag.
- [12] E Hinton and D R J Owen (1979). *An Introduction to Finite Element Computations*. Pineridge Press, UK.
- [13] P K Jimack (1992). *On Steady and Large Time Solutions of the Semi-Discrete Moving Finite Element Equations for One-Dimensional Diffusion Equations*. IMA J. Num. Anal., 12, 545–564.
- [14] P K Jimack (1993). *A Best Approximation Property of the Moving Finite Element Method*. School of Computer Studies Report 93.35, University of Leeds. (Submitted to SIAM J. Num. Anal.)
- [15] P K Jimack and A J Wathen (1991). *Temporal Derivatives in the Finite Element Method on Continuously Deforming Grids*. SIAM J. Num. Anal., 28, 990–1003.
- [16] I W Johnson, A J Wathen and M J Baines (1988). *Moving Finite Element Methods for Evolutionary Problems. II. Applications*. J. of Comp. Phys., 79, 270–297.
- [17] J E Marsden and T J R Hughes (1983). *Mathematical Foundations of Elasticity*. Prentice-Hall, NJ.
- [18] K Miller and R Miller (1981). *Moving Finite Elements, Part I*. SIAM J. Num. Anal., 18, 1019–1032.
- [19] K Miller (1981). *Moving Finite Elements, Part II*. SIAM J. Num. Anal., 18, 1033–1057.
- [20] A C Mueller (1983). *Continuously Deforming Finite Element Methods for Transport Problems*. Ph.D. Thesis, University of Austin, Texas. Unpublished.
- [21] A C Mueller and G F Carey (1985). *Continuously Deforming Finite Elements*. Int. J. Num. Meth. Eng., 21, 2099–2126.
- [22] Numerical Algorithms Group Limited (1993) *The NAG Fortran Library Manual – Mark 14*.
- [23] J W Tang and D J Turke (1977). *Characteristics of Optimal Grids*. Comput. Meth. Appl. Mech. Eng., 11, 31–37.
- [24] A J Wathen and M J Baines (1985). *On the Structure of the Moving Finite Element Equations*. IMA J. Num. Anal., 5, 161–182.
- [25] J Z Zhu and O C Zienkiewicz (1988). *Adaptive Techniques in the Finite Element Method*. Comm. Appl. Num. Methods, 4, 197–204.